Central European Journal of Energetic Materials, **2014**, *11*(4), 553-573
ISSN 2353-1843

A Comprehensive Study of the Electrostatic Discharge Sensitivity and Chargeability of Tris(carbohydrazide)zinc Perchlorate

Zhimin LI [1], Dandan ZENG [2], Zunning ZHOU [1], Mingrui ZHOU [1, 3], Tonglai ZHANG [1,*], Huisheng HUANG [4, **], Jianguo ZHANG [1], Li YANG [1]

[1] State Key Laboratory of Explosion Science and Technology, Beijing Institute of Technology, Beijing 100081, PR China
[2] Laboratory for High Temperature Gas Dynamics, Institute of Mechanics, Chinese Academy of Sciences, Beijing 100190, PR China
[3] China Academy of Launch Vehicle Technology, Beijing 100076, PR China
[4] Chongqing Key Laboratory of Inorganic Special Functional Materials, College of Chemistry and Chemical Engineering, Yangtze Normal University, Chongqing 408100, PR China
*E-mail: *ztlbit@bit.edu.cn, **h.s.huang@hotmail.com*

Abstract: Most primary explosives are non-conductors, easily accumulate charge when contacting with and separating from other materials, and are sensitive to electrostatic discharge (ESD). In order to reduce the number of accidents caused by ESD initiation of primary explosives, studies on their electrostatic hazards are necessary. This work presents comprehensive experimental results of electrostatic discharge sensitivity and chargeability of tris(carbohydrazide)zinc perchlorate (ZnCP) under different conditions. The influences of the testing conditions, of devices, particle size, ambient temperature and relative humidity on the electrostatic discharge sensitivity and chargeability have been investigated in detail, and the quantitative regression equations obtained.

Keywords: primary explosive, tris(carbohydrazide)zinc perchlorate, electrostatic discharge sensitivity, chargeability

1 Introduction

Electrostatic charging is a common phenomenon in many fields and has attracted considerable interest [1-8]. The hazards of granular materials caused by static charge have been extensively studied, as dust explosions in pneumatic conveying systems and ESD ignited energetic materials [6, 9-18]. It is well known that electrostatic charges may be generated when two particles of different materials come into contact and then separate. This is the so-called "triboelectric charging". The mechanism is related to the contact potential difference (CPD) between the contacting surfaces, generally regarded as a critical driving force of charge transfer [19, 20]. Most explosives are nonconductors. In the processes of preparation and transportation, they easily accumulate static charge. If the potential is enough to cause breakdown in the medium, the ESD may initiate a terrible accident [21-24].

Commonly, the electrostatic hazard of granular explosives is characterized by ESD sensitivity and chargeability, both of which are relative empirical values, and may be influenced by many factors, including the test method and conditions, the physical form of the sample and the ambient temperature and relative humidity [25-29]. Li and Wang studied comprehensively the ESD sensitivity of lead styphnate, black powder and hydrogen, investigated the effects of various fundamental factors on the ignition energy and found the optimum ignition conditions [25]. Sumner *et al.* have done much work on the ignition by ESD of primary explosives, such as lead azide and lead styphnate, as well as the effects of temperature and relative humidity on the accumulation of electrostatic charge on fabrics and primary explosives [30-33]. Raha *et al.* investigated in detail the development of static charge on explosives [34, 35]. Roux *et al.* reported that the spark energy transfer mechanisms are different for pure HMX and the explosive, *i.e*. HMX, containing 1% graphite, investigated the influence of electrode shape, grain size and shape, as well as environmental conditions on ESD sensitivity [27]. Talawar *et al.* reported the ESD sensitivity of some primary explosives, in terms of the zero ignition probability energy, and correlations between spark energy and thermal, detonation and mechanical properties [9]. The present work was focused on the ESD sensitivity and chargeability of an energetic coordination compound.

Energetic coordination compounds of transition metal perchlorates, such as the well known CP (pentaammine (5-cyano-2H-tetrazolato-N^2) cobalt(III) perchlorate) and BNCP (tetraammine-*cis*-bis(5-nitro-2H-tetrazolato-N^2) cobalt(III) perchlorate), have aroused considerable interest in recent years due to their excellent performance as primary explosives [36-38]. The ligands

which have been most studied are 5-nitrotetrazole [39, 40], 1,5-diaminotetrazole [41-44], imidazole [45], ethylenediamine [46] and carbohydrazide (CHZ) [47, 48]. In 2004, Talawar *et al.* studied the synthesis, characterization and performance evaluation of transition metal complexes of carbohydrazide, and revealed that tris(carbohydrazide)nickel perchlorate (NiCP) and CoCP are superior detonants as compared to mercuric fulminate and service lead azide, in terms of low vulnerability to initiation by mechanical and thermal stimuli [49]. Tris(carbohydrazide)cadmium perchlorate (CdCP) has been investigated by Zhang *et al.* [50-51], Sa *et al.* [52] and has been well used as a primary explosive in China since 1999. Since 2001, Zhang's group have done much work on preparative techniques, morphological control and application performances of ZnCP [53-56]. At present, tris(carbohydrazide)zinc perchlorate (ZnCP) is widely used in industrial detonators in China. It is readily prepared and exhibits excellent initiating ability. Moreover, the central atom, being Zn rather than heavy metals, reduces the hazard to operators and the environment.

2 Experimental

2.1 Preparation of tris(carbohydrazide)zinc perchlorate

ZnCP was obtained by reaction of CHZ with zinc perchlorate according to the reported route [51] as shown in Figure 1. Samples of various particle sizes were obtained by sieving, the particle size (d) of the sample between two sieves being defined as the median of the two meshes, in microns.

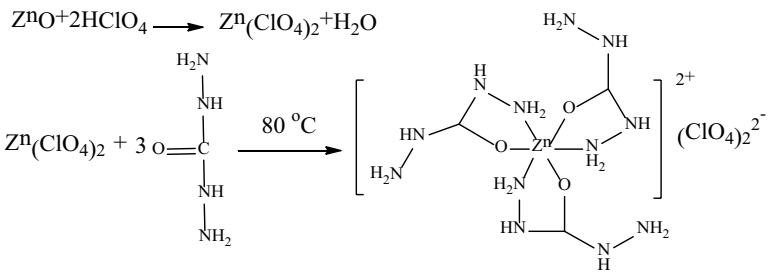

Figure 1. The synthetic route for ZnCP.

2.2 Electrostatic discharge sensitivity test

A schematic diagram of the ESD sensitivity tester is shown in Figure 2. The charging circuit consists of a high voltage power generator and a bank of capacitors. After the capacitors have been charged, a vacuum discharge switch

insulates them from the charging circuit and connects them to the discharge circuit, which contains the ignition device in the form of a needle electrode. The sample is placed in a holder that is secured to the grounded base electrode. The electrode gap is measured with a dial gauge. The energy is given by the formula $E = 0.5CV^2$, where C is the capacitance of the capacitor, in farads (F), and V is the charge voltage, in volts (V). A series of 30 samples was tested using the up and down method, and the ESD sensitivity (E_{50}) for 50 percent probability of ignition was calculated according to the usual Bruceton formula [52].

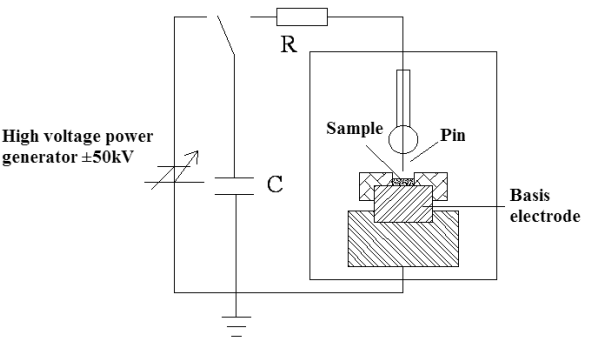

Figure 2. Schematic diagram of the electrostatic discharge sensitivity tester.

2.3 Chargeability test

The "chargeability (Q)" is defined herein as the accumulated electrostatic charge on unit mass of the primary explosive after friction with other materials. The chargeability testing system was constructed as shown in Figure 3. Figure 4 displays a typical graph of static charge (Q_0), voltage (U) and weight (W) against time. A 5 g sample was placed in the sample box, poured into the flume and allowed to flow through it. The sample became charged in this manner by friction with the flume and flow into the Faraday cage. Flumes of different materials were used to simulate the triboelectrification between the granular primary explosive and various materials of the devices used in the processes of preparation and application. Five different kinds of flume materials were used in this work, including stainless steel, fabroil, aluminum, conductive rubber and shellac painted kraft flume. The tilt angle of the flume could be changed from 0 to 90°, and the length of the flume could be changed from 20 to 100 cm. Seven tests were carried out for each condition, and the results were averaged.

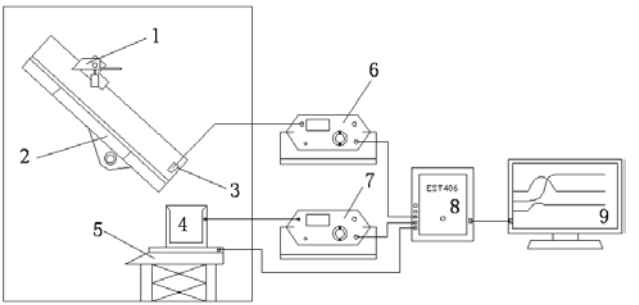

Figure 3. Schematic diagram of the chargeability testing system.
1 – sample box; 2 – flume; 3 – voltage probe; 4 – Faraday cage; 5 – digital balance; 6 – vibration capacitor electrometer; 7 – digital charge meter; 8 – computer data gathering and processing system; 9 – computer.

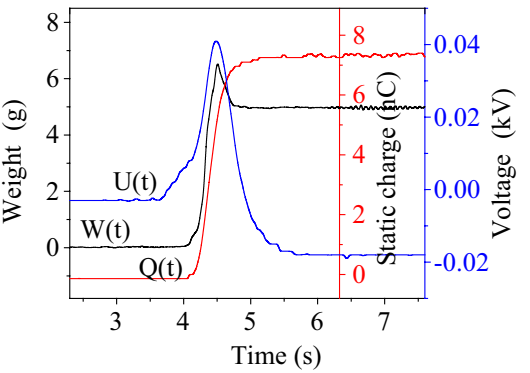

Figure 4. Typical *Q/U/W-t* curves from the chargeability testing device.

3 Results and Discussion

3.1 Parametric study of the electrostatic discharge sensitivity test

For ZnCP, the measured magnitude of the ESD sensitivity varies with its particle size and the testing conditions. The testing conditions, including the electrode geometry and material, the gap between the electrodes, electropositive discharge or electronegative discharge, the bank of capacitors and the additional resistor in the discharge circuit, and furthermore the ambient temperature and relative humidity. Thus, the determined data were obtained on a specific experimental stand, which should be associated with the magnitude of the ESD sensitivity.

A different shape and material of the electrode will alter the area and the electrical intensity of the ESD. Here, a steel needle and column electrodes were used. The gap between the electrodes is a key factor affecting the ESD character and the initiation ability. The E_{50} values of ZnCP with different electrode gaps were obtained (C = 0.22 μF, R = 100 kΩ, electronegative discharge), and are shown in Figure 5. The E_{50} decreases with decreasing electrode gap, and the linear relationship can be described by Equation (1), where *gap* is the magnitude of the electrode gap, in millimetres. The statistical significance values, including the correlation coefficient, degrees of freedom, residual sum of squares, adjusted R-square, F-values and Prob>F, were obtained and are listed in Table 1.

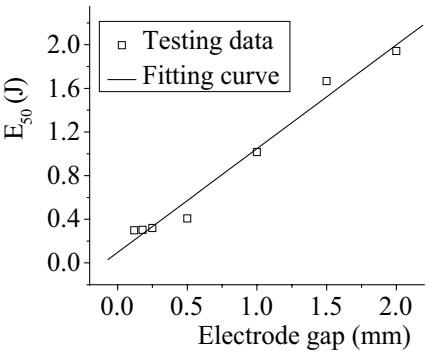

Figure 5. Variation of E_{50} of ZnCP versus electrode gap, C = 0.22 μF, R = 100 kΩ.

Equation (1): $E_{50} = 0.0956 + 0.9516\ gap$

ZnCP can be ignited by an electronegative discharge with an E_{50} of 0.25 J (C = 0.22 μF, R = 100 kΩ, V_{50} = -1.5 kV, R is an additional resistance in the discharge circuit). However, when using an electropositive discharge, ZnCP cannot be ignited by 62.5 J (C = 0.22 μF, R = 100 kΩ, V = 25 kV). This may be attributed to the high density of electrons around the needle electrode causing ZnCP to decompose quickly when ignited by an electronegative discharge.

Figure 6 shows the variation of E_{50} versus the capacitance of various capacitors; the resistance in the discharge circuit was 100 kΩ and the electrode gap was 0.18 mm. Along with the increase in the capacitance, the value of E_{50} initially decreased and then increased. The relation between E_{50} and the capacitance can be fitted by Equation (2), where C is the capacitance of the capacitor. In the fitted curve, a minimum E_{50} was found corresponding to the optimum ignition capacitance of ZnCP under these conditions. If the capacitance

Table 1. The statistical significance values of the regression equations

No.	Equation	Correlation coefficient	Degrees of freedom	Residual sum of squares	Adj. R-Square	F value	Prob>F
1	E_{50}=0.0956+0.9516g	0.99	5	0.0609	0.9754	238.4313	2.0681×10^{-5}
2	E_{50}=1.5130-12.2697C+27.7419C^2	0.96	3	0.0348	0.8862	20.4752	0.0178
3	Q=4.5114-0.2469θ+0.0027θ^2	0.96	4	0.0422	0.9001	28.0427	0.0044
4	Q=-9.530+0.6189θ-0.0065θ^2	0.93	4	0.4080	0.8108	13.8566	0.0159
5	Q=-2.5879+0.1857θ-0.0020θ^2	0.94	4	0.0445	0.8275	15.3888	0.0132
6	Q=-6.7743+0.4291θ-0.0045θ^2	0.97	4	0.0866	0.9136	32.7269	0.0033
7	Q=-8.2007+0.4657θ-0.0048θ^2	0.98	4	0.0383	0.9569	67.6733	8.2400×10^{-4}
8	Q=0.5614-0.03407L	-0.98	5	0.1091	0.9610	148.9259	6.5333×10^{-5}
9	Q=-0.2214+0.0944L	-0.99	5	0.5692	0.9732	218.9677	2.5488×10^{-5}
10	Q=0.3179+0.0272L	-0.99	5	0.0278	0.9841	372.0423	6.9087×10^{-6}
11	Q=-0.3421+0.0699L	-0.99	5	0.2179	0.9812	313.9272	1.0508×10^{-5}
12	Q=-0.1600+0.0648L	-0.98	5	0.4970	0.9513	118.2273	1.1427×10^{-4}
13	Q=13.8334-3.0556f-3.2382v	0.98	4	0.0279	0.9341	43.4912	0.0019
14	Q=-19.4038+3.9749f+2.4753v	0.94	4	0.3493	0.8380	16.5214	0.0117
15	Q=-9.7954+2.3384f+2.4753v	0.96	4	0.0300	0.8837	23.7934	0.0060
16	Q=-11.0554+2.2785f+2.6592v	0.98	4	0.0485	0.9516	59.9986	0.0010
17	Q=-12.4728+2.4202f+3.0422v	0.97	4	0.0639	0.9283	39.8178	0.0023
18	E_{50}=0.2704+4.7628×10^{-5}exp (d/27.6196)	0.99	3	0.0047	0.9860	354.7284	2.7324×10^{-4}
19	Q=0.3795+17.6951exp (-d/34.7671)	0.99	3	0.0195	0.9816	293.2958	3.62957×10^{-4}
20	E_{50}=0.4052-0.0049T	-0.98	1	4.1607×10^{-5}	0.9325	28.6185	0.1176
21	Q=3.3143-0.1136T	-1	1	0.0014	0.9825	113.5043	0.0599
22	E_{50}=-0.0744+0.0063H	1	2	1.4880×10^{-5}	0.9982	1689.3022	5.9146×10^{-4}
23	Q=2.8698-0.0230H	0.97	1	0.0015	0.8945	17.9606	0.1475

The confidence level for the test parameters was 5%.

of the capacitor is not at the optimum value, part of the discharge energy is wasted. Previous studies on lead styphnate by Li Guoxiang demonstrated the optimum ignition conditions [25]. Michel Roux reported that the behaviour of the secondary explosive HMX is consistent with an optimum ignition capacitance [27]. Here, the energetic coordination compound ZnCP also has an optimum ignition capacitance.

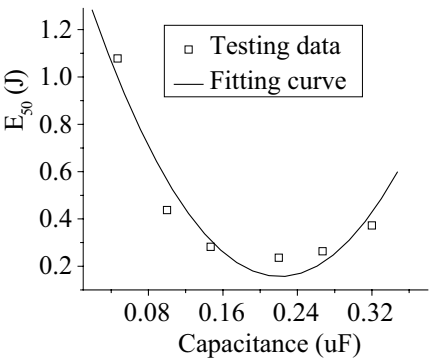

Figure 6. Variation of E_{50} of ZnCP versus capacitance, with a 100 kΩ resistor in the discharge circuit; gap length 0.18 mm.

Equation (2): $E_{50} = 1.5130 - 12.2697\ C + 27.7419\ C^2$

An additional resistor in the discharge circuit extends the discharge time of the capacitor and consumes part of the energy. A longer discharge time influences the ESD ignition behaviour of explosives; some energetic complexes can be easily ignited under these conditions, but others are more sensitive to a shorter discharge. The E_{50} of energetic complexes of several transition metal perchlorates (Mn/Ni/Cd/Zn) with carbohydrazide, (tris(carbohydrazide)manganese perchlorate (MnCP), tris(carbohydrazide)nickel perchlorate (NiCP), tris(carbohydrazide) cadmium perchlorate (CdCP) and ZnCP), were obtained with and without an additional resistor (100 kΩ) in the discharge circuit ($C = 0.22$ μF, $gap = 0.18$ mm, electronegative discharge). The E_{50} values of MnCP, NiCP, CdCP and ZnCP were 2.86, 9.31, 1.43 and 0.25 J, respectively, with the resistor in the discharge circuit. However, if there were no resistor, the magnitudes of the E_{50} values were 8.14, 0.09, 0.44 and 12.83 J, respectively. The four complexes have the similar structures. In their decomposition processes, the collapse of the ring of the coordinated carbohydrazide and dissociative ClO_4^- may be similar, but the catalytic abilities of the central cations are different, and play an important role in the explosion or combustion. When stimulated by ESD with a resistor (100 kΩ)

in the discharge circuit, the transition metal perchlorate energetic complexes with carbohydrazide respond with combustion, but, if there is no resistor, they explode rapidly. The order of the electrostatic discharge sensitivity of the complexes tested with a short discharge is Ni (0.09 J) > Cd (0.44 J) > Mn (8.14 J) > Zn (12.83 J), which is similar to the order of their burning rates (64, 44, 6 and 8 $cm \cdot s^{-1}$ at 10 MPa, respectively) [53]. The burning rate of the Ni complex is the largest, so, in the case of a short-time discharge, the deflagration to detonation transition (DDT) occurs easily, and the Ni complex can be easily ignited to explosion. The order of the 5 s delay explosion temperatures of the energetic complexes is Zn (325 °C) > Cd (330 °C) > Mn (339 °C) > Ni (362 °C), which is similar to the order of their electrostatic discharge sensitivities (Zn (0.25 J) > Cd (1.43 J) > Mn (2.86 J) > Ni (9.31 J)), when tested with a resistor in the discharge circuit.

3.2 Analysis of the test chargeability process

Triboelectrification between granular samples and the flume is affected by the friction between the sample and the flume, as well as the speed of sample flow in the flume, which are related to the friction coefficient. To obtain the friction coefficient, the time of sample flow in the flume was measured by two probes in the flume. According to formula (1), the friction coefficients (μ) between ZnCP and stainless steel, fabroil, aluminum, conductive rubber and shellac painted kraft flumes were obtained as 0.28, 0.56, 0.36, 0.62 and 0.60, respectively. A 1 gram sample was taken to calculate the friction according to formula (2). The speed of flow is described as the speed of the sample flowing out of the flume, and is obtained by formula (3). Tables 2 and 3 list the chargeability, test time, friction coefficient, friction and speed of flow of ZnCP with various lengths and angles of the different flumes.

$$\left.\begin{aligned} a &= g\sin\theta - \mu g\cos\theta \\ L &= \frac{1}{2}at^2 = \frac{1}{2}(g\sin\theta - \mu g\cos\theta)t^2 \end{aligned}\right\} \Rightarrow \mu = \frac{\sin\theta - \dfrac{2L}{gt^2}}{\cos\theta} \tag{1}$$

$$f = \mu g\cos\theta \tag{2}$$

$$v = \sqrt{2L(g\sin\theta - \mu g\cos\theta)} \tag{3}$$

In formulae (1), (2) and (3): a is the acceleration, $m \cdot s^{-2}$; g is the acceleration due to gravity, 9.8 $m \cdot s^{-2}$; θ is the angle of the flume, °; μ is the friction coefficient; L is the length of the flume, cm; t is the time of sample flow in the flume; f is friction between the sample and flume, N; v is the speed of the sample flowing out of the flume, $m \cdot s^{-1}$.

Table 2. Chargeability of ZnCP and related parameters with various flume angles (flume length 60 cm)

θ, [°]	t (tested) [ms]	μ	t (calculated) [ms]	f, [N]	v, [m·s^{-1}]	Q, [nC·g^{-1}]
Stainless steel						
35	668	0.37	663	2.89	1.81	-0.83
40	539	0.29	578	2.703	2.078	-1.15
45	466	0.2	520	2.495	2.307	-1.36
50	450	0.25	479	2.268	2.507	-1.23
55	452	0.38	447	2.024	2.684	-0.92
60	405	0.24	423	1.764	2.84	-0.75
65	392	0.26	403	1.491	2.978	-0.41
Fabroil						
35	977	0.54	1033	4.496	1.162	4.17
40	825	0.6	757	4.204	1.586	4.66
45	693	0.64	627	3.881	1.913	5.45
50	594	0.65	549	3.528	2.185	5.41
55	502	0.58	496	3.148	2.42	4.76
60	449	0.52	457	2.744	2.625	3.84
65	412	0.44	428	2.319	2.806	3.56
Aluminum						
35	828	0.48	663	2.89	1.81	1.38
40	614	0.42	578	2.703	2.078	1.74
5	522	0.36	520	2.495	2.307	1.83
50	434	0.18	4789	2.268	2.507	1.69
55	428	0.26	447	2.024	2.684	1.48
0	436	0.44	423	1.764	2.84	1.34
65	388	0.22	403	1.491	2.978	1.12
Conductive rubber						
35	925	0.53	1365	4.977	0.879	2.65
40	825	0.6	854	4.654	1.405	3.16
45	693	0.64	675	4.296	1.778	3.63
50	607	0.67	577	3.906	2.079	3.32
55	522	0.64	514	3.485	2.335	3.07
60	462	0.58	469	3.038	2.557	2.66
65	416	0.47	436	2.568	2.753	2.13
Shellac painted kraft						
35	1109	0.58	1221	4.817	0.983	2.26
40	798	0.59	818	4.504	1.468	2.69

θ, [°]	t (tested) [ms]	μ	t (calculated) [ms]	f, [N]	v, [m·s^{-1}]	Q, [nC·g^{-1}]
45	686	0.63	658	4.158	1.824	3.21
50	568	0.6	567	3.78	2.115	3.18
55	502	0.58	508	3.373	2.363	2.86
60	449	0.52	465	2.94	2.58	2.54
65	416	0.47	433	2.485	2.771	1.92

Table 3. Chargeability of ZnCP and related parameters with various flume lengths (flume angle 45 °)

L, [cm]	t (tested) [ms]	μ	t (calculated) [ms]	f, [N]	v, [m·s^{-1}]	Q, [nC·g^{-1}]
Stainless steel						
30	336	0.23	367.8	2.495	1.631	-0.62
40	436	0.39	424.7	2.495	1.884	-0.77
50	453	0.3	474.8	2.495	2.106	-0.99
60	466	0.2	520.2	2.495	2.307	-1.36
70	542	0.31	561.8	2.495	2.492	-1.81
80	565	0.28	600.6	2.495	2.664	-2.37
90	603	0.29	637.1	2.495	2.825	-2.46
Fabroil						
30	428	0.53	443.6	3.881	1.353	2.92
40	502	0.54	512.2	3.881	1.562	3.12
50	543	0.51	572.7	3.881	1.746	4.39
60	612	0.54	627.3	3.881	1.913	5.45
70	694	0.58	677.6	3.881	2.066	6.85
80	732	0.57	724.4	3.881	2.209	7.09
90	813	0.61	768.3	3.881	2.343	8.26
Aluminum						
30	392	0.44	367.8	2.495	1.631	1.09
40	421	0.35	424.7	2.495	1.884	1.46
50	448	0.28	474.8	2.495	2.106	1.74
60	522	0.36	520.2	2.495	2.307	1.83
70	610	0.46	561.8	2.495	2.492	2.28
80	623	0.41	600.6	2.495	2.664	2.46
90	639	0.36	637.1	2.495	2.825	2.78
Conductive rubber						
30	469	0.61	477.3	4.296	1.257	1.84
40	554	0.62	551.2	4.296	1.451	2.33

L, [cm]	t (tested) [ms]	μ	t (calculated) [ms]	f, [N]	v, [m·s^{-1}]	Q, [nC·g^{-1}]
50	620	0.62	616.2	4.296	1.623	3.16
60	693	0.64	675.1	4.296	1.778	3.63
70	785	0.67	729.1	4.296	1.92	4.91
80	832	0.67	779.5	4.296	2.053	5.27
90	852	0.64	826.8	4.296	2.177	5.82
Shellac painted kraft						
30	475	0.62	465.3	4.158	1.29	1.86
40	561	0.63	537.2	4.158	1.489	2.77
50	616	0.62	600.6	4.158	1.665	2.96
60	686	0.63	658	4.158	1.824	3.21
70	746	0.64	710.7	4.158	1.97	4.22
80	823	0.66	759.8	4.158	2.106	5.21
90	852	0.64	805.8	4.158	2.234	5.86

Figure 7 shows the relationship between Q for ZnCP and the tilt angle of the flume. The regression equations of Q on the tilt angle of the flume can be described by Equations (3-7) for a stainless steel flume, a fabroil flume, an aluminum flume, a conductive rubber flume, and a shellac painted kraft flume, respectively, where Q is the chargeability (nC·g^{-1}), and θ is the tilt angle of the flume (°). The statistical significance values are given in Table 1.

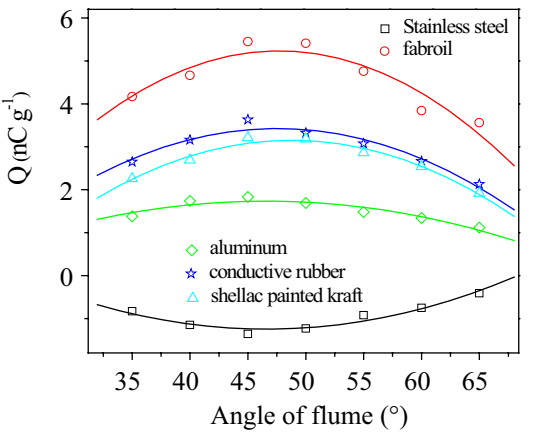

Figure 7. Dependence of chargeability of ZnCP on the tilt angle of the flume; flume length 60 cm.

Equation (3): $Q = 4.5114 - 0.2469\theta + 0.0027\theta^2$

Equation (4): $Q = -9.530 + 0.6189\theta - 0.0065\theta^2$
Equation (5): $Q = -2.5879 + 0.1857\theta - 0.0020\theta^2$
Equation (6): $Q = -6.7743 + 0.4291\theta - 0.0045\theta^2$
Equation (7): $Q = -8.2007 + 0.4657\theta - 0.0048\theta^2$

The effects of the length of flume on Q for ZnCP are shown in Figure 8. The chargeability increases linearly with increasing length of the flume, and can be described by Equations (8-12) for a stainless steel flume, a fabroil flume, an aluminum flume, a conductive rubber flume, and a shellac painted kraft flume, respectively, where L is the length of the flume (cm). The statistical significance values are given in Table 1.

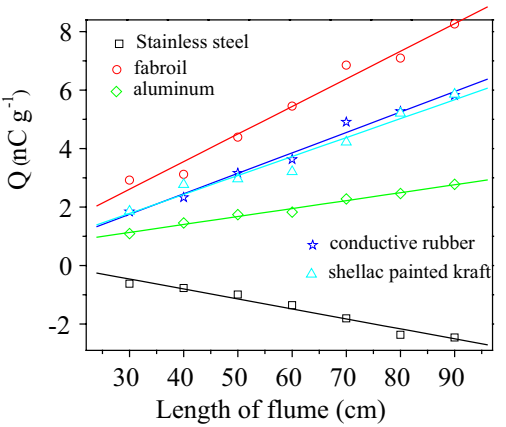

Figure 8. Dependence of chargeability of ZnCP on the length of the flume; flume tilt angle 45°.

Equation (8): $Q = 0.5614 - 0.03407\ L$
Equation (9): $Q = -0.2214 + 0.0944\ L$
Equation (10): $Q = 0.3179 + 0.0272\ L$
Equation (11): $Q = -0.3421 + 0.0699\ L$
Equation (12): $Q = -0.1600 + 0.0648\ L$

In order to investigate the effects of friction and flow speed on chargeability, the length of the flume was keep constant and the tilt angle was varied. Based on the data in Table 1, a binary linear regression model was constructed between the chargeability and the friction and flow speed. The model can be described by Equations (13-17) for a stainless steel flume, a fabroil flume, an aluminum flume, a conductive rubber flume and a shellac painted kraft flume, respectively,

where f is friction (N) and v is the flow speed ($m \cdot s^{-1}$). The chargeability increases with increasing friction and flow speed. The predicted chargeability of ZnCP with different friction and flow speeds from these models corresponds well with the experimental values, as shown in Figure 9.

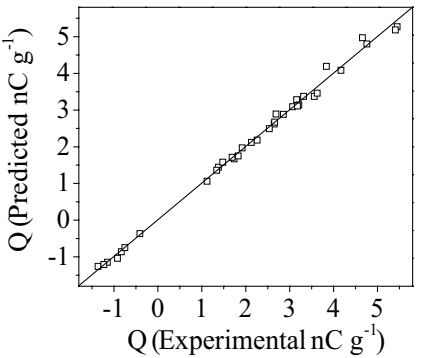

Figure 9. Plot of predicted chargeability values against experimental ones.

Equation (13): $Q = 13.8334 - 3.0556\,f - 3.2382\,v$
Equation (14): $Q = -19.4038 + 3.9749\,f + 2.4753\,v$
Equation (15): $Q = -9.7954 + 2.3384\,f + 2.4753\,v$
Equation (16): $Q = -11.0554 + 2.2785\,f + 2.6592\,v$
Equation (17): $Q = -12.4728 + 2.4202\,f + 3.0422\,v$

3.3 Effects of particle size

Figure 10 shows the dependence of electrostatic discharge sensitivity and chargeability for ZnCP on particle size. The relations are fitted by the exponential Equations (18) and (19), where d is the particle size (μm). The statistical significance values are given in Table 1. The E_{50} increased and the chargeability decreased with increasing particle size of ZnCP. Smaller ZnCP particles are more sensitive to electrostatic spark. This can be explained by the smaller particles being able to completely absorb the electrostatic energy. The smaller particles have a larger specific surface, and this results the fully friction and increased chargeability.

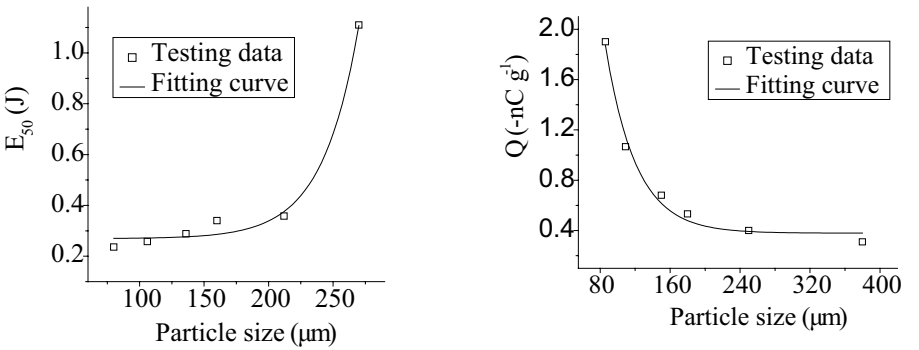

Figure 10. Dependence of electrostatic discharge sensitivity (C = 0.22 μF, R = 100 kΩ, g = 0.18 mm) and chargeability (stainless steel flume, 60 cm, 45 °) of ZnCP on particle size.

Equation (18): $E_{50} = 0.2704 + 4.7628 \times 10^{-5} \exp(d/27.6196)$
Equation (19): $Q = 0.3795 + 17.6951 \exp(-d/34.7671)$

3.4 Effects of ambient temperature and relative humidity

The effects of ambient temperature and relative humidity on the electrostatic discharge sensitivity and chargeability of ZnCP were investigated. The results are shown in Figures 11 and 12, respectively. Both the electrostatic discharge sensitivity and the chargeability exhibit a linear correlation with ambient temperature and relative humidity. The linear equations for the dependence of electrostatic discharge sensitivity (E_{50}/J) and chargeability (Q/nC·g^{-1}) on the temperature (T/°C)and relative humidity (H/%), derived by regression analysis, are expressed as Equations (20-23).

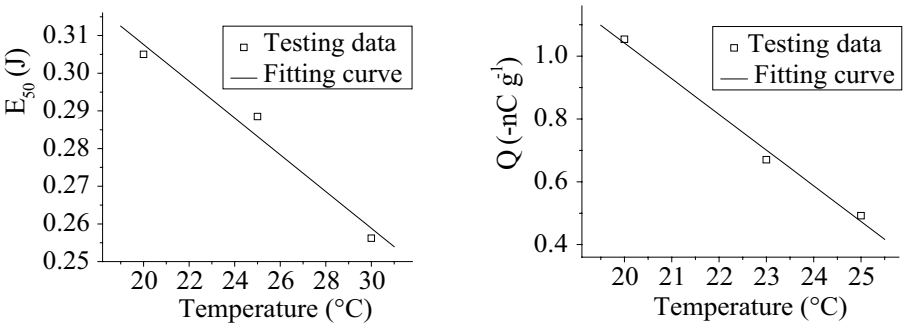

Figure 11. Dependence of electrostatic discharge sensitivity (C = 0.22 μF, R = 100 kΩ, g = 0.18 mm) and chargeability (stainless steel flume, 60 cm, 45 °) of ZnCP on temperature.

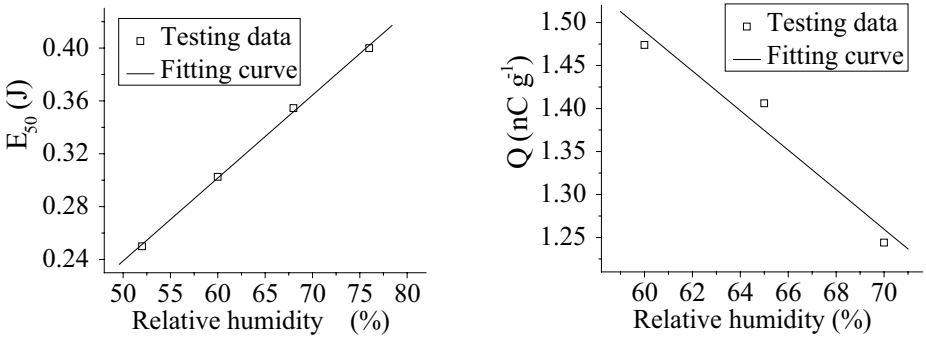

Figure 12. Dependence of electrostatic discharge sensitivity (C = 0.22 μF, R = 100 kΩ, g = 0.18 mm) and chargeability (kraft flume, 60 cm, 45 °) of ZnCP on relative humidity.

Equation (20): $E_{50} = 0.4052 - 0.0049\ T$
Equation (21): $Q = 3.3143 - 0.1136\ T$
Equation (22): $E_{50} = -0.0744 + 0.0063\ H$
Equation (23): $Q = 2.8698 - 0.0230\ H$

The value of E_{50} increases with decreasing temperature and increasing relative humidity. In a cryodrying environment, ZnCP readily generates and accumulates electrostatic charge. Linear correlations were also reported by Li *et al.* in their study on the effects of temperature and relative humidity on the electrostatic discharge sensitivity of black powder [25].

4 Conclusion

Electrostatic discharge sensitivity and chargeability of tris(carbohydrazide) zinc perchlorate were comprehensive tested under different conditions, and the influences of various factors were investigated in detail.

The variation of the E_{50} of ZnCP versus the electrode gap can be described by: $E_{50} = 0.0956 + 0.9516\ gap$, *i.e.* E_{50} decreases with decreasing electrode gap. The relation between the E_{50} of ZnCP and the capacitance can be fitted by: $E_{50} = 1.5130 - 12.2697\ C + 27.7419\ C^2$. The relation between the E_{50} of ZnCP and its particle size can be described by: $E_{50} = 0.2692 + 5.6683 \times 10^{-5} \exp(d/28.1188)$. The linear equations for the dependence of the E_{50} of ZnCP on temperature (T/°C) and relative humidity (H/%) can be described by: $E_{50} = 0.4052 - 0.0049\ T$, $E_{50} = -0.0744 + 0.0063\ H$, respectively.

The friction coefficients between ZnCP and aluminum and stainless steel flumes were determined as 0.36 and 0.28, respectively. The relationships between the Q of ZnCP and the tilt angle and length of the flume can be fitted by: $Q = -2.8598 + 0.1759\theta - 0.0019\theta^2$ and $Q = -2.0.5614 + 0.0341\ L$, respectively, for a stainless steel flume. A binary linear regression model was found for the chargeability of ZnCP and the friction and flow speed: $Q = 10.6320 - 2.8794\ f - 2.5654\ v$ for a stainless steel flume. The relations between Q and the particle size of ZnCP can be described by: $Q = 1.8974 + 88.4758\exp(-d/34.7670)$. The linear equations for the dependence of the Q of ZnCP on temperature and relative humidity can be described by: $Q = 16.5716 - 0.5682\ T$ and $Q = 14.3483 - 0.1150\ H$, respectively.

Acknowledgement

We gratefully acknowledge financial support from the National Basic Research Program of China, the Natural Science Foundation of Chongqing (Grant No. cstc2011jjA50013), the Scientific and Technological Research Program of Chongqing Municipal Education Commission (Grant No. KJ111310) and the Doctoral Candidate Innovation Research Support Program by the Science and Technology Review (kjdb201001-2).

5 References

[1] Ma C.Q., Zhao S.L., Huang G., Anti-static Charge Character of the Plasma Treated Polyester Filter Fabric, *J. Electrostat.*, **2010**, *68*(2), 111-115.

[2] Thomas S.W., Vella S.J., Kaufman G.K., Whitesides G.M., Patterns of Electrostatic Charge and Discharge in Contact Electrification, *Angew. Chem. Int. Ed.*, **2008**, *47*(35), 6654-6656.

[3] Liao C.C., Hsiau S.S., Huang T.Y., The Effect of Vibrating Conditions on the Electrostatic Charge in a Vertical Vibrating Granular Bed, *Powder Technol.*, **2011**, *208*(1), 1-6.

[4] Lacks D., Duff N., Kumar S., Nonequilibrium Accumulation of Surface Species and Triboelectric Charging in Single Component Particulate Systems, *Phys. Rev. Lett*., **2008**, *100*(18), 188305(1-4).

[5] Janes A., Chaineaux J., Carson D., LeLore P.A., MIKE 3 versus HARTMANN Apparatus: Comparison of Measured Minimum Ignition Energy (MIE), *J. Hazard. Mater*., **2008**, *152*(1), 32-39.

[6] Nomura T., Satoh T., Masuda H., The Environment Humidity Effect on the Tribo-charge of Powder, *Powder Technol.*, **2003**, *135-136*, 43-49.

[7] Lu M., Zhao S.X., Chen J., Measurement and Analysis of the Frictional Static

Electricity Characteristics of Composite RDX, *Chinese J. Energ. Mater*., **2008**, *16*(6), 708-711.

[8] LaMarche K.R., Liu X., Shah S.K., Shinbrot T., Glasser B.J., Electrostatic Charging During the Flow of Grains from a Cylinder, *Powder Technol*., **2009**, *195*(2), 158-165.

[9] Talawar M.B., Agrawal A.P., Anniyappan M., Wani D.S., Bansode M.K., Gore G.M., Primary Explosives: Electrostatic Discharge Initiation, Additive Effect and Its Relation to Thermal and Explosive Characteristics, *J. Hazard. Mater.*, **2006**, *137*(2), 1074-1078.

[10] Keshavarz M.H., Theoretical Prediction of Electric Spark Sensitivity of Nitroaromatic Energetic Compounds Based on Molecular Structure, *J. Hazard. Mater.*, **2008**, *153*(1-2), 201-206.

[11] Keshavarz M.H., Pouretedal H.R., Semnani A., Reliable Prediction of Electric Spark Sensitivity of Nitramines: A General Correlation with Detonation Pressure, *J. Hazard. Mater.*, **2009**, *167*(1-3), 461-466.

[12] Turker L., Contemplation on Spark Sensitivity of Certain Nitramine Type Explosives, *J. Hazard. Mater.*, **2009**, *169*(1-3), 454-459.

[13] Zeman S., New Aspects of Initiation Reactivities of Energetic Materials Demonstrated on Nitramines, *J. Hazard. Mater.*, **2006**, *132*(2-3), 155-164.

[14] Bane S.P.M., Shepherd J.E., Kwon E., Day A.C., Statistical Analysis of Electrostatic Spark Ignition of Lean H_2/O_2/Ar Mixtures, *Int. J. Hydrogen Energy*, **2011**, *36*(3), 2344-2350.

[15] Yao J., Wang C.H., Granular Size and Shape Effect on Electrostatics in Pneumatic Conveying Systems, *Chem. Eng. Sci.*, **2006**, *61*(12), 3858-3874.

[16] Nifuku M., Katoh H., A Study on the Static Electrification of Powders During Pneumatic Transportation and the Ignition of Dust Cloud, *Powder Technol*., **2003**, *135-136*, 234-242.

[17] Bates W.D., Kosowski B.M., Gotzmer C., Development of Passivated Pyrophoric Metal Powders (Hafnium and Zirconium) with Reduced Electrostatic Discharge (ESD) Sensitivity, *Combus. Energ. Mater*., **2002**, *1029*, 985-993.

[18] Yu X.H., Surface Treatment of PETN via Decreasing Static Electricity, *Chinese J. Explos. Propellants*, **2003**, *26*(4), 55-56.

[19] Hogue M.D., Buhler C.R., Calle C.I., Matsuyama T., Luo W., Groop E.E., Insulator-insulator Contact Charging and Its Relationship to Atmospheric Pressure, *J. Electrostat*., **2004**, *61*(3-4), 259-268.

[20] Matsusyama T., Yamamoto H., Impact Charging of Particulate Materials, *Chem. Eng. Sci*., **2006**, *61*(7), 2230-2238.

[21] Sun D.Q., Gao M., Hao X.M., Gao Z.L., Study on the Hazard and Countermeasures of Static Electricity in the Initiating Explosive Device Production, *Explosive Materials*, **2009**, *38*(3), 22-24.

[22] Li H.J., Ji Z.J., Yang H.L., Discusions on the Safety Technique of Electrostatic in the Field of Initiating and Chemical Engineering, *Technology Foundation of National Defence*, **2009**, *4*, 50-53.

[23] Cao H.F., Wang G.L., Evaluation of Electrification Safety of Powder Emulsion Explosives, *Mining & Metallurgy*, **2004**, *13(3)*, 9-12.
[24] Bao T., Zhang W., Review on Electrostatic Hazards of Composite Solid Propellant, *Chinese J. Energ. Mater*., **2010**, *18*(4), 460-466.
[25] Li G.X., Wang C.Y., Comprehensive Study on Electric Spark Sensitivity of Ignitable Gases and Explosive Powders, *J. Electrostat*., **1982**, *11*(3), 319-332.
[26] Larson T.E., Dimas P., Hannaford C.E., Electrostatic Sensitivity Testing of Explosives at Los-Alamos, *Institute of Physics Conference Series*, **1991**, *118*, 107-117.
[27] Roux M., Auzanneau M., Brassy C., Electric Spark and ESD Sensitivity of Reactive Solids (Primary or Secondary Explosive, Propellant, Pyrotechnics) Part I: Experimental Results and Reflection Factors for Sensitivity Test Optimization, *Propellants Explos. Pyrotech*., **1993**, *18*, 317-324.
[28] Auzanneau M., Roux M., Electric Spark and ESD Sensitivity of Reactive Solids (Primary or Secondary Explosive, Propellant, Pyrotechnics) Part II: Energy Transfer Mechanisms and Comprehensive Study on E_{50}, *Propellants Explos. Pyrotech*., **1995**, *20*, 96-101.
[29] Darin S., Douglas O., Andrew B.B., Electrostatic Discharge Ignition of Energetic Materials, *Propellants Explos. Pyrotech*., **1998**, *23*, 34-42.
[30] Hammant B.L., Sumner J.F., Wyatt R.M.H., Assessing the Electrostatic Behaviour of Clothing for Use in an Explosive Environment, *J. Electrostat*., **1981**, *10*, 343-350.
[31] Sumner J.F., Ignition of Primary Explosives by Electrostatic Discharges, *DECHEMA Monographien*, **1974**, *72*(1370-1409), 409-417.
[32] Cleves A.C., Sumner J.F., Wyatt R.M.H., Effect of Temperature and Relative Humidity on the Accumulation of Electrostatic Charges on Fabrics and Primary Explosives, *Static Elec., Proc. Conf., 3rd*, **1971**, 226-233.
[33] Wyatt R.M.H., Moore P.W.J., Adams G.K., Sumner J.F., The Ignition of Primary Explosives by Electric Discharges, *Proc. Royal Soc. London, Series A, Mat. and Phys. Sciences*, **1958**, 246, 189-196.
[34] Raha K., Chhabra J.S., Static Charge Development on Explosives, *Def. Sci. J.*, **1991**, *41*(1), 21-25.
[35] Raha K., Chhabra J.S., Static Charge Development and Impact Sensitivity of High Explosives, *J. Hazard. Mater.*, **1993**, *34*(3), 385-391.
[36] Wojewodka A., Belzowski J., Wilk Z., Stas J., Energetic Characteristics of Transition Metal Complexes, *J. Hazard. Mater.*, **2009**, *171*(1-3), 1175-1177.
[37] Talawar M.B., Agrawal A.P., Chhabra J.S., Ghatak C.K., Asthana S.N., Rao K.U.B., Studies on Nickel Hydrazinium Nitrate (NHN) and Bis-(5-nitro-2*H* tetrazolato-N^2) Tetraamino Cobalt(III) Perchlorate (BNCP): Potential Lead-free Advanced Primary Explosives, *J. Sci. Ind. Res.*, **2004**, *63*(8), 677-681.
[38] Blachowski T.J., Burchett J., Ostrowski P.P., U.S. Navy Characterization of Two Energetic Materials, CP and BNCP, *38th AIAA Joint Propulsion Conference & Exhibit*, Indianapolis, **2002**, 7-10 July.
[39] Shang J., Zhang J.G., Zhang T.L., Huang H.S., Zhang S.W., Shu Y.J., Theoretical

Study of Energetic Complexes (III): Bis-(5-nitro-2H-tetrazolato-N-2)tetraammine Cobalt(III) Perchlorate (BNCP) and Its Transition Metal (Ni/Fe/Cu/Zn) Perchlorate Analogues, *Chinese J. Energ. Mater*., **2012**, *30*(7), 1624-1630.

[40] Talawar M.B., Agrawal A.P., Asthana S.N., Energetic Co-ordination Compounds: Synthesis, Characterization and Thermolysis Studies on Bis-(5-nitro-2H-tetrazolato-N-2)tetraammine Cobalt(III) Perchlorate (BNCP) and Its New Transition Metal (Ni/Cu/Zn) Perchlorate Analogues, *J. Hazard. Mater.*, **2005**, *120*(1-3), 25-35.

[41] Cui Y., Zhang J.G., Zhang T.L., Yang L., Zhang J., Hu X.C., Synthesis, Structural Investigation, Thermal Decomposition Mechanism and Sensitivity Properties of an Energetic Compound $[Cd(DAT)_6](ClO_4)_2$ (DAT = 1,5-diaminotetrazole), *J. Hazard. Mater.*, **2008**, *160*(1), 45-50.

[42] Shang J., Zhang J.G., Cui Y., Zhang T.L., Shu Y.J., Yang L., Synthesis, Crystal Structure, and Properties of an Energetic Compound [Zn(1,5-diaminotetrazole)$_6$] $(ClO_4)_2$, *Acta Chim. Sinica*, **2010**, *68*(3), 233-238.

[43] Qi S.Y., Li Z.M., Zhou Z.N., Cu Y.I, Zhang G.T., Zhang T.L., Zhang J.G., Yang L., Crystal Structure, Thermal Decomposition Behaviours and Sensitivity Properties of a Novel Energetic Compound $[Co(DAT)_6]$ $(ClO_4)_2$, *Chinese J. Energ. Mater*., **2011**, *29*(1), 59-64.

[44] Qi S.Y., Zhang J.G., Zhang T.L., Cui Y., Yang L., Yu K. B., Shu Y.J., Synthesis, Crystal Structure, Thermal Behaviour and Sensitivity Properties of New Energetic Compound $[Mn(DAT)_6](ClO_4)_2$, *Chem. J. Chinese U.*, **2009**, *30*(10), 1935-1939.

[45] Li Z.M., Zhou Z.N., Zhang T.L., Tang Z., Yang L., Zhang J.G., Energetic Transition Metal (Co/Cu/Zn) Imidazole Perchlorate Complexes: Synthesis, Structural Characterization, Thermal Behavior and Non-isothermal Kinetic Analyses, *Polyhedron*, **2012**, *44*(1), 59-65.

[46] Singh G., Felix S.P., Pandey D.K., Studies on Energetic Compounds – Part 37: Kinetics of Thermal Decomposition of Perchlorate Complexes of some Transition Metals with Ethylenediamine, *Thermochim. Acta*, **2004**, *411*(1), 61-71.

[47] Huang H.S., Zhang T.L., Zhang J.G., Wang L.Q., A Screened Hybrid Density Functional Study on Energetic Complexes: Cobalt, Nickel And Copper Carbohydrazide Perchlorates, *J. Hazard. Mater.*, **2010**, *179*(1-3), 21-27.

[48] Sun Y.H., Zhang T.L., Zhang J.G., Yang L., Qiao X.J., Decomposition Kinetics of Manganese Tris(Carbohydrazide) Perchlorate (MnCP) Derived from the Filament Control Voltage of the T-Jump/FTIR Spectroscopy, *Int. J. Therm. Sci.*, **2006**, *45*, 814-818.

[49] Talawar M.B., Agrawal A.P., Chhabra J.S., Asthana S.N., Studies on Lead-free Initiators: Synthesis, Characterization and Performance Evaluation of Transition Metal Complexes of Carbohydrazide, *J. Hazard. Mater.*, **2004**, *113*(1-3), 57-65.

[50] Zhang T.L., Wei Z.R., Lu C.H., Zhang J.G., Research on the Primary Explosive GTG, *Explosive Materials*, **1999**, *28*(3), 16-19.

[51] Li L.M., Yang A.M., Zhang T.L., Zhang J.G., Qiao X.J., Studies on Plain Detonator of GTG Primary Explosive, *Explosive Materials*, **2004**, *33*(4), 16-20.

[52] Sa G., Cao W.J., Shu B.Y., Application of GTG Primary Explosive to Industrial Detonator, *Explosive Materials*, **2001**, *30*(1), 15-19.
[53] Sun Y.H., Zhang T.L., Zhang J.G., Qiao X.J., Yang L., Flash Pyrolysis Study of Zinc Carbohydrazide Perchlorate Using T-jump/FTIR Spectroscopy, *Combust. Flame*, **2006**, *145*, 643-646.
[54] Liu R., Qi S.Y., Zhang T.L., Zhou Z.N., Yang L., Zhang J.G., Morphological Control of Zinc Tricarbohydrazide Perchlorate Crystals: Theoretical and Experimental Study, *Chinese Sci. Bull.*, **2013**, *58*(16), 1892-1896.
[55] Huang H.S., Zhang T.L., Zhang J.G., Wang L.Q., Density Functional Theoretical Study of Transition Metal Carbohydrazide Perchlorate Complexes, *Chem. Phys. Lett.*, **2010**, *487*(4-6), 200-203.
[56] Zhang Z.G., Zhang J.G., Zhang T.L., Yang Y.M., Preparation Technique and Explosive Properties of $[Zn(CHZ)_3](ClO_4)_2$, *Chin. J. Energ. Mater. (Hanneng Cailiao)*, **2001**, *9*(2), 49-52.
[57] Dixon W.J., Mood A.M., The Statistical Sign Test, *J. Am. Stat. Assoc*., **1946**, *41*(236), 557-566.
[58] Fogelzang A.E., Sinditskii V.P., Egorshev V., Serushkin V.V., Effect of Structure of Energetic Materials on Burning Rate, in Decomposition, Combustion, and Detonation Chemistry of Energetic Materials, *MRS Proceedings*, **1995**, *418*, 151-161.